Dimensional matching *vs*. induced-fit distortions. Binding affinities of planar and curved polyaromatic hydrocarbons with a tetra-gold metallorectangle

Susana Ibáñez[a] and Eduardo Peris[a]*

Abstract: A tetragold(I) rectangle-like metallocage containing two pyrene-bis-imidazolylidene ligands and two carbazolyl-bis-alkynyl linkers is used for the encapsulation of a series of polycyclic aromatic hydrocarbons (PAHs), including corannulene. The molecular structures of the host:guest complexes formed are described. The binding affinities obtained for the encapsulation of anthracene, pyrene, triphenylene and perylene in CH_2Cl_2 are found to be very high ($5.2 > \log K > 5.6$), due to an excellent host:guest dimensional matching. For coronene and corannulene, the affinities are lower than the expected ones, due to the distortions produced in the structure of the receptor. The molecular structure of the host:guest complex formed with corannulene shows that the molecule of the guest is compressed, while the host is expanded, therefore showing an unusual case of artificial mutual induced-fit arrangement.

Introduction

The well-defined sizes and shapes, together with the rigidity of supramolecular coordination complexes (SCCs),[1] offer a wide variety of applications via host-guest interactions. These interactions can be tuned by altering the size and shape of the building blocks. The modification of the properties shown by guest molecules encapsulated in the cavities of supramolecular structures have attracted the interest of chemistry researchers during the last three decades.[2] The most efficient receptors are those designed by nature, like enzymes, which are conformationally flexible so that they can adapt to respond to the shape of specific guest molecules.[3] Such induced-fit conformational change is now used as a general strategy to maximize the binding between artificial hosts and guests,[4] but the examples in which induced-fit binding has been used for enhancing efficiently host-guest affinity are very few. This is because most synthetic hosts are rigid structures with little flexibility, thus the conformational changes observed are always smaller than those shown in biological receptors. Even rarer is to find examples of artificial receptors in which both host and guest mutually induce the organization of each other.[5] Such mutual induced-fit in artificial systems are of great interest, because they can constitute a way for controlling the properties of dynamic molecules, and have the potential to be used as strategy for stabilizing conformationally modified molecules not available out of their confinements.

During the last few years, we have reported a series of supramolecular coordination compounds based on a pyrene-bis-imidazolylidene ligand.[6] Despite the unique photophysical properties of pyrene, this molecule has rarely been introduced in the structure of SCCs,[7] probably because most supramolecular coordination complexes are based on a more or less limited number of Werner-type ligands. The introduction of pyrene into the structure of a SCC also brings the advantage that it can magnify the affinity of the metal complex toward planar aromatic guests by favoring $\pi-\pi$-stacking interactions. Not surprisingly, Nietschke and co-workers recently demonstrated that the incorporation of large aromatic panels into the structure of metallocages brings about more effective hosts for the encapsulation of polyaromatic guests.[7c]

We also used a carbazolyl-bis-alkynyl linker that behaves as a very convenient linker for the preparation of metallotweezers and metallocages.[8] Our main interest was to use these supramolecular coordination compounds (SCCs) as receptors for polycyclic aromatic hydrocarbons (PAHs). Our interest was motivated by the fact that these organic molecules are hazardous materials that have gathered significant environmental concern.[9] It should be noted that the use of SCCs for the encapsulation of PAHs has provided a large number of examples for the last 15 years,[7c, 10] but the search for more efficient metallocage-based receptors continuous to be a challenge because the binding affinities found are still far from those shown by the most efficient pure organic-based systems.[11]

We also used our metallosupramolecular assemblies for the encapsulation of fullerenes, and found that our cages were able to adapt their shape to the size of the fullerene (C_{60} or C_{70}), by an induced-fit conformational change of the host.[6b, 6c] This induced-fit change mainly involved the bending of the pyrene panels of the cage in order to yield a concave surface that maximizes the face-to-face overlap with the convex surface of these three-dimensional guests. Given the flexibility shown by our supramolecular cages containing the pyrene-bis-imidazolylidene ligand, we thought that we could use the same type of building block for preparing a molecular cage in which we could not only trap planar polycyclic aromatic hydrocarbons but also curved ones. Corannulene is a C_{5v} symmetric bowl-shaped PAH that can be regarded as a hydrogen terminated cap of fullerene C_{60}.[12] It is probably its bowl-shaped structure that makes corannulene a very challenging guest to trap, due to the lack of supramolecular cages with suitable surfaces for establishing an effective face-to-face $\pi-\pi$ overlap. In 2014, Siegel and Stoddart used a synthetic receptor that combined two extended bipyridinium units joined end-to-end by two *para*-xylene linkers ($ExBox^{4+}$),[11c] which resulted very efficient for the encapsulation of corannulene.[13] The authors found that the encapsulated corannulene showed significant reduction of the energy barrier for the concave-convex inversion, although the planarization of the bowl-shaped guest was insignificant. One year later, Fujita and co-workers described the significant flattening of corannulene upon inclusion within a trigonal prismatic metallosupramolecular assembly.[14] The

[a] Dr. S. Ibáñez and Prof. E. Peris
Institute of Advanced Materials (INAM). Centro de Innovación en Química Avanzada (ORFEO-CINQA). Universitat Jaume I. Av. Vicente Sos Baynat s/n. Castellón. E-12071. Spain.
Email: eperis@uji.es
Supporting information for this article is given via a link at the end of the document.

compression of corannulene was facilitated by the effective donor-acceptor interactions shown within the cavity of the cage when naphthalene diimide was used as a co-guest within the structure. With these precedents in hand, we now report the preparation of a tetra-gold metallorectangle that combines two pyrene-bis-imidazolylidene ligands with two carbazol-bis-alkynyl linkers. As will be described, this supramolecular cage is especially designed for encapsulating a variety of PAHs, including corannulene, for which an unsusual type of mutual induced-fit arrangement is observed.

Results and Discussion

Preparation of tetragold metallorectangle and related host:guest complexes. The metallorectangle **2** was obtained by following the synthetic procedure shown in Scheme 1. The deprotonation of di-*tert*-butyl-diethynyl-carbazole with NaOH in refluxing methanol followed by the addition of the pyrene-bis-imidazolydene-gold(I) complex **1**,[15] afforded the tetra-Au(I) compound **2** in 71% yield after purification. When the reaction was carried out in the presence of one equivalent of an electron-rich PAH (anthracene, pyrene, triphenylene, perylene, coronene or corannulene), the corresponding inclusion complexes (PAH)@**2** were obtained. In all cases, except for the reaction with anthracene (yield 64%), the product yields were significantly increased (82-91%), most likely due to the templation effect[16] produced by the addition of the electron-rich PAH. All compounds **2** and (PAH)@**2** were characterized by NMR spectroscopy and gave satisfactory elemental analysis. The Diffusion Ordered NMR spectra (DOSY) of all (PAH)@**2** complexes show that all proton resonances display the same diffusion coefficient in $CDCl_3$ for each host:guest species, indicating that all PAH molecules are associated with the metallorectangle forming a single assembly (see ESI for details).

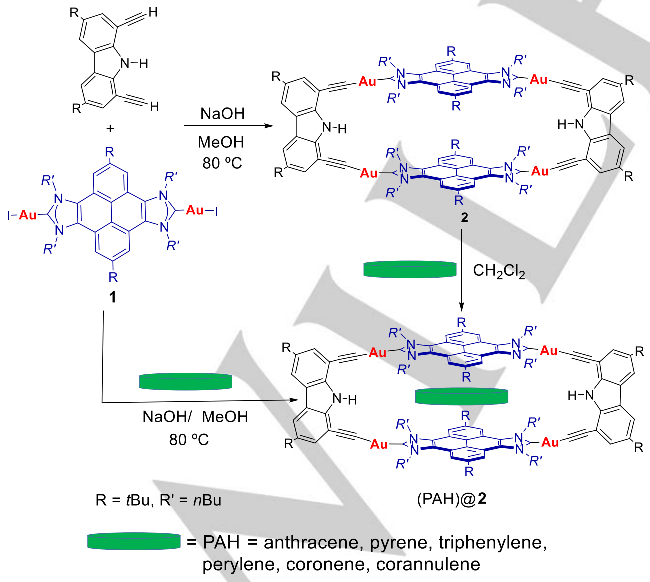

Scheme 1. Synthesis of metallorectangle **2**, and the inclusion complexes (PAH)@**2**.

Molecular structures of the complexes. Single crystals suitable for X-ray diffraction studies of **2** and some of its inclusion complexes [(anthracene)@**2**, (pyrene)@**2,** (perylene)@**2**, (coronene)@**2** and (corannulene)@**2**] were obtained by slow diffusion of hexane into a concentrated solution of the complexes in dichloromethane or chloroform. The molecular structures of these complexes are shown in Figure 1.

The molecular structure of 'empty' complex **2** (Figure 1a) consists of a tetragold-rectangle with two cofacial pyrene-bis-imidazolylidene ligands and two carbazolyl-bis-alkynyls that constitute the shorter sides of the rectangle. The average distance between the gold atoms bound to the same carbazoyl-bis-alkynyl ligand is 6.555 Å, while the distance between the gold centers bound by the same di-carbene ligand measures 13.144 Å. The distance between the planes formed by the cofacial pyrene units is 7.214 Å. The molecular structures of (anthracene)@**2**, (pyrene)@**2**, (perylene)@**2** and (coronene)@**2** are qualitatively similar to that shown by 'empty' **2**, with the difference that a planar PAH molecule is trapped inside the cavity of the metallorectangle. This makes that some of the metric parameters of the cage are slightly changed. For example, the distance between the two parallel pyrene units of the cage are 7.098, 6.935, 6.987 and 6.936 Å, for (anthracene)@**2**, (pyrene)@**2**, (perylene)@**2** and (coronene)@**2**, respectively. This indicates that the cage compresses upon encapsulation of the PAH guest, and that this compression becomes larger for complexes containing the three larger PAH molecules, probably because the π-stacking interaction becomes more efficient. In all cases, the centroid of the PAH molecules is perfectly aligned with the centroids of the pyrene panels of the cage. The structure of (coronene)@**2** shows a deviation of the face-to-face alignment of the two planes formed by the pyrene panels of the host, to afford an offset, slipped parallel-displaced conformation. This can be quantified by comparing the angles between the planes defined by the carbazolyl moieties, and the plane of the pyrene units of the cage. This angle ranges between 87-90º for the empty cage and the cage with the encapsulated smaller PAH molecules, and goes down to 75.41º for (coronene)@**2**. The structure of (coronene)@**2** (Figure 1e) also shows that the encapsulation of coronene produces a sterically constrained environment, due to the close proximity between the edge of the coronene molecule and the *tert*-butyl groups of the pyrene units. As can be observed in the molecular structure, the pyrene panels are bent along its longer axis, so that the separation between the *tert*-butyl groups and the edge of the coronene is increased in order to minimize the steric repulsion. As will be described below, these structural perturbations have important implications in the binding constant found for the association between coronene and **2**.

The molecular structure of (corannulene)@**2** (Figure 1f) shows significant differences due to the bowl-shaped nature of the guest. The distance between the parallel pyrene panels is 7.618 Å, thus approximately 0.6 Å larger than the average related distance for all other four molecular structures mentioned above. The distance between the gold atoms bound to the same carbazolyl-di-alkynyl ligand is 6.628 Å, very similar to the related distance found for the rest of the molecular structures, thus indicating that the separation between the pyrene panels is produced mainly by a distortion of the pyrene-bis-imidazolydene ligands. In fact, the pyrene-bis-imidazolydene ligands are bent, and form a concave inner surface

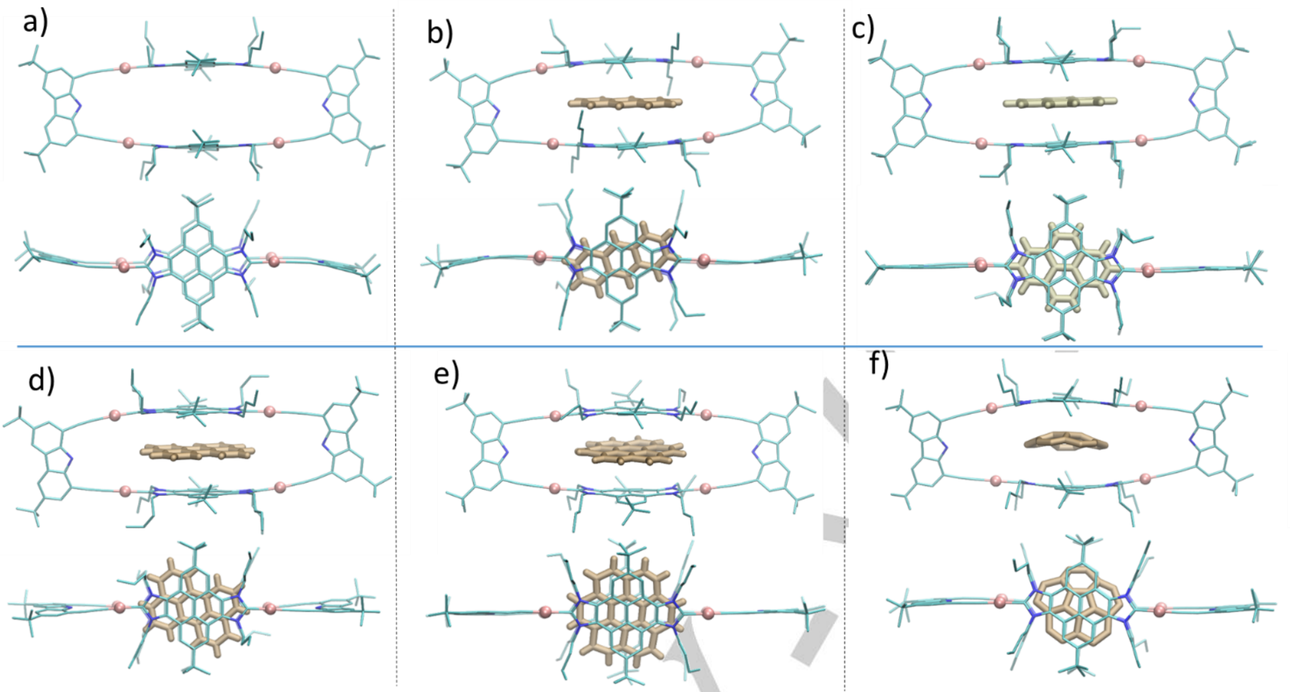

Figure 1. Two perspectives of the molecular structures of **2** (a), (anthracene)@**2** (b), (pyrene)@**2**, (c) (perylene)@**2** (d) (coronene)@**2** (e), and (corannulene)@**2** (f), obtained from single crystal X-ray diffraction studies.

that maximizes the face-to-face contact with the convex surface of the guest. On the other hand, the pyrene panel close to the convex surface of corannulene is not bent in a convex manner, as one should expect for maximizing the π–π-stacking interaction with the guest. Rather than that, this panel is also bent in a concave manner, therefore this part of the molecule deviates from the optimum π–π-stacking overlap. This situation makes that the metallocage looks like 'inflated' compared to the structure of **2**, and to the rest of the structures of the metallocage with the encapsulated planar PAHs. The bowl-depth (BD) of the encapsulated corannulene is 0.74 Å, therefore significantly reduced compared to the structure of free corannulene (BD = 0.87 Å).[17] This compression is more significant than the one found by Siegel and co-workers for the encapsulation of corannulene in ExBox^{4+},[13] but much lower than the one described by Fujita for the encapsulation of this bowl-shaped PAH in a trigonal prismatic metallocage with a co-guest (BD = 0.56 Å).[14] Noteworthy, the distance between the centroid of the central five-membered ring of the guest and the plane formed by the pyrene unit of the host is 3.04 Å, which is significantly shorter than the sum of the van der Waals radii for sp^2-hybridized carbon atoms (3.4-3.6 Å). This explains why the distance between the parallel panels of the metallocage (7.62 Å) is significantly shorter than the one expected from the sum of the van der Waals radii of the stacks and the BD of corannulene (2x3.5 + 0.74 = 7.74 Å). This is a very interesting point given that shorter π–π stacking leads to stronger charge transfer, a property that is highly pursued in the design of molecular electronic devices.[18]

We DFT calculated (wB97XD/def2TZVP) the energy cost of the compression of the corannulene molecule, by following the transformation of the molecule along the concave-convex inversion path, from the D_{5h} flat transition state to the C_{5v} bowl-shaped ground state. According to these calculations, the energy cost for compressing corannulene from BD = 0.87 to 0.74 Å is 0.77 kcal/mol (0.77 kcal/mol above the ground-state structure). This energy can also be regarded as the decrease of the energy barrier for the bowl-to-bowl inversion process, which we DFT calculated as $\Delta G^{\neq}$ = 10.98 kcal/mol for the free corannulene (therefore 10.21 kcal/mol for the flattened structure). This energy barrier can be further decreased if we consider the plausible 'extra' stabilization of the transition state within the cage. This is likely due to an optimization of the surface overlap of the host and the guest, which maximizes the π-stacking interaction when the guest is flat, as previously found by Siegel and co-workers.[13]

Determination of binding affinities. In order to quantify the extent of the binding between **2** and the PAH guests, we performed a series of titrations to determine the association constants for the 1:1 complexes formed. We started by performing ^{1}H NMR titrations, and observed that in all cases the addition of the PAH guest induced the upfield shifting of the signals due to the protons of the pyrene units of **2**, thus evidencing that the formation of the inclusion complexes showed fast kinetics on the NMR timescale. However, these titrations were unsuitable for providing reliable results, because the binding constants were found to exceed the limits for providing accurate values (NMR titrations are only valid for determining constants below 10^4-10^5 M^{-1}).[19] Consequently, for the determination of the association constants, Uv-Vis. titrations were carried out. These were performed in CH_2Cl_2, at room temperature and at a constant concentration of **2** (10^{-6} M). Complex **2** shows high-energy absorptions between 250-350 nm, attributed to pyrene-centered ligand-to-ligand charge transfer transitions. Upon addition of the PAH guests, new bands appeared in the same region, which are attributed to charge transfer transitions between the polyaromatic guests and the pyrene units of the host. Based on the changes observed, the constants were determined by global fitting analysis,[19] by processing the data using a 1:1 stoichiometric model. The results indicate that the binding affinities of the PAH guests are in the order coronene≈corannulene << anthracene < pyrene < triphenylene < perylene, as can be observed from the values shown in Table 1. For hosts with very large portals, it has been shown that the affinity between the host and the guest generally follows a linear trend of increasing $\log K_a$ values with increasing number of π-electrons in the guests.[6d, 11a, 11c] This can be explained because as the π-electronrichness of the guest increases, the $\pi-\pi$-stacking interaction between the host and the guest becomes more effective, and therefore the association constant becomes larger. In our case, this linear trend is clearly observed when the binding affinities of anthracene, pyrene, triphenylene and perylene are compared (Figure 3). It should be noted that, to our knowledge, the binding affinities for the four smaller PAH molecules (anthracene, pyrene, triphenylene and perylene), are among the highest found for a metal-containing receptor, and compare well with the best organic-based hosts.[11a, 11c] These large affinities are a consequence of the excellent dimensional matching between the planar guests and the rectangular metallacycle, together with the effective $\pi-\pi$-stacking established between the aromatic guests and the pyrene panels of the receptor. Interestingly, the binding affinities found are about two orders of magnitude larger compared to the ones that we recently reported for a trigonal-prismatic hexa-gold(I) receptor with a triphenylene-tris-NHC ligand.[8b]

Table 1. Association constants (M^{-1}) for the complexation of **2** with PAHs.

Entry	Guest	K_{11}	$\log K_{11}$
1	anthracene	(1,71± 0,03) x10^5	5,23
2	pyrene	(2,2± 0,1) x10^5	5,34
3	triphenylene	(3,4± 0,2) x10^5	5,53
4	perylene	(4,4± 0,2) x10^5	5,64
5	coronene	(3,8± 0,1) x10^4	4,57
6	corannulene	(3,2± 0,1) x10^4	4,50

[a] K_{11} values calculated by global nonlinear regression analysis.[19] Titrations carried out by Uv-vis spectroscopy, using constant concentrations of **2** (host) of 10^{-3} mM in CH_2Cl_2 at 298 K. Errors refer to the non-linear regression fittings.

In the case of coronene, the experimental value obtained is much lower than the value estimated by the regression analysis obtained from plotting $\log K_a$ *vs.* number of π-electrons of the guest ($\log K_a$ = 4.57, compared to $\log K_a$ = 6.93 as expected from the linear regression). By comparing the experimental association constant, and the one expected from the linear regression, a ΔG value of 1.83 kcal/mol is obtained. This energy loss that lowers the overall affinity of coronene towards the metallocage can be ascribed to the sterically strained situation that arises from the encapsulation of the large molecule of coronene, as reflected by the structural changes in **2** upon complexation. As can be observed from the molecular structure of coronene@**2**, the structure of the metallorectangle shows a significant structural distortion compared to empty box **2**. As discussed above, this structural change is mainly taking place at the pyrene units of the host, which bend along the axis defined by the *tert*-butyl groups in order to minimize the steric repulsion between these bulky moieties and the rim of the large polyaromatic guest. This structural distortion must have an energy cost, but also renders a situation in which the pyrene panels of the receptor slightly deviate from the optimum face-to-face overlap with the surface of the guest to afford the most efficient $\pi-\pi$-stacking interaction.

The binding constant of corannulene with **2** is 3.2 x 10^4 M^{-1}. Perylene has the same number of π-electrons as corannulene (20), but unlike corannulene, perylene is flat. The K_{11} value of perylene is 4.4 x 10^5 M^{-1}. The energy loss that can be calculated from the different binding constants is 1.54 kcal/mol. In this case, this energy loss cannot be solely attributed to the strain generated in the components on complexation, which includes the energy cost that involves the compression of corannulene. In this case we also need to take into account two important factors: i) the difference in the solvation energies of perylene and corannulene and, ii) the fact that the π-stacking interaction between the host and the guest becomes less effective for this bowl-shaped molecule, as one of the pyrene panels of the metallocage clearly deviates from the optimum face-to-face overlap, as reflected in the molecular structure of (corannulene)@**2** (Figure 1f).

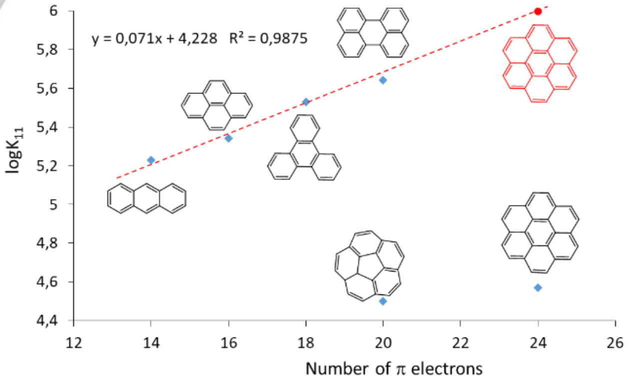

Figure 3. Plot of the association constants (K_{11}) in CH_2Cl_2 between **2** and the number of π-electrons of the PAHs used in this study. The red dot in the plot represents the expected K_{11} value for coronene as estimated from the linear regression.

Conclusions

In conclusion, we prepared a tetragold metallocage that behaves as a very effective receptor of a variety of polycyclic aromatic hydrocarbons. Despite its apparent two-dimensional structure, this metallocage shows very high binding affinities towards PAH molecules, and competes well with other three-dimensional supramolecular structures, traditionally considered as more suitable for the encapsulation of these type of organic guests. The large binding affinities found are due to the incorporation of two cofacial pyrene panels separated by $\approx$7Å, thus providing the optimum conditions for guest recognition by π–π-stacking interactions. The cage shows larger binding affinities towards the smaller PAHs, because the excellent dimensional matching allows that the encapsulation takes place at a minimum energy cost due to the negligible structural distortions of host and guests. The affinity towards coronene is significantly reduced due to the steric constraints shown in the resulting host:guest complex, which produce the structural distortion of the host with the concomitant loss of efficiency of the π–π-stacking interaction between host and guest. The encapsulation of corannulene is accompanied by a significant compression of the bowl-shaped molecule of the guest and the concomitant expansion of the host metallocage. This mutual induced-fit arrangement has an energy cost, which in part justifies the reduced binding affinity of corannulene compared to the expected one according to the linear trend shown in Figure 3. The lack of an effective π–π-stacking interaction over the convex surface of the guest also contributes to the reduction of the binding affinity. It is worth mentioning that the compression of corannulene upon encapsulation in a receptor has been described only twice. The compression observed in our work is significantly larger than that observed by Siegel and Stoddart for the encapsulation of corannulene in ExBox^{4+},[11c] but smaller than that observed by Fujita using a trigonal-prismatic palladium-cornered host in the presence of a heteroguest.[14] We believe that our system is simpler than the latter one, because the cushion-like behavior of corannulene is produced without the need of using heteroguests for maximizing the donor-acceptor interaction between the host for corannulene.

Acknowledgements

We gratefully acknowledge financial support from the Ministerio de Ciencia y Universidades (PGC2018-093382-B-I00) and the Universitat Jaume I (UJI-B2017-07 and UJI-A2017-02). We are grateful to the Serveis Centrals d'Instrumentació Científica (SCIC-UJI) for providing with spectroscopic facilities. We would like to thank Dr. Macarena Poyatos, for her valuable help in the refinement of the crystal structure, and for providing very useful thoughts for the developement of this study. We also thank Prof. Dmitri Gusev (Wilfrid Laurier University) for the DFT calculations.

Keywords: N-heterocyclic carbenes • Gold • Supramolecular coordination complexes • host-guest • PAHs

[1] a) N. Sinha, F. E. Hahn, *Acc. Chem. Res.* **2017**, *50*, 2167-2184; b) C. Lescop, *Acc. Chem. Res.* **2017**, *50*, 885-894; c) L. Chen, Q. Chen, M. Wu, F. Jiang, M. Hong, *Acc. Chem. Res.* **2015**, *48*, 201-210; d) M. M. J. Smulders, I. A. Riddell, C. Browne, J. R. Nitschke, *Chem. Soc. Rev.* **2013**, *42*, 1728-1754; e) M. L. Saha, S. De, S. Pramanik, M. Schmittel, *Chem. Soc. Rev.* **2013**, *42*, 6860-6909; f) G. Kumar, R. Gupta, *Chem. Soc. Rev.* **2013**, *42*, 9403-9453; g) P. D. Frischmann, M. J. MacLachlan, *Chem. Soc. Rev.* **2013**, *42*, 871-890; h) P. Thanasekaran, R. T. Liao, Y. H. Liu, T. Rajendran, S. Rajagopal, K. L. Lu, *Coord. Chem. Rev.* **2005**, *249*, 1085-1110; i) M. Fujita, M. Tominaga, A. Hori, B. Therrien, *Acc. Chem. Res.* **2005**, *38*, 369-378; j) F. Wurthner, C. C. You, C. R. Saha-Moller, *Chem. Soc. Rev.* **2004**, *33*, 133-146; k) T. R. Cook, P. J. Stang, *Chem. Rev.* **2015**, *115*, 7001-7045; l) T. R. Cook, Y.-R. Zheng, P. J. Stang, *Chem. Rev.* **2013**, *113*, 734-777; m) R. Chakrabarty, P. S. Mukherjee, P. J. Stang, *Chem. Rev.* **2011**, *111*, 6810-6918; n) D. W. Zhang, T. K. Ronson, J. R. Nitschke, *Acc. Chem. Res.* **2018**, *51*, 2423-2436; o) A. J. McConnell, C. S. Wood, P. P. Neelakandan, J. R. Nitschke, *Chem. Rev.* **2015**, *115*, 7729-7793; p) P. Ballester, M. Fujita, J. Rebek, Jr., *Chem. Soc. Rev.* **2015**, *44*, 392-393.

[2] a) A. Galan, P. Ballester, *Chem. Soc. Rev.* **2016**, *45*, 1720-1737; b) M. Ziegler, J. L. Brumaghim, K. N. Raymond, *Angew. Chem. Int. Ed.* **2000**, *39*, 4119-4121.

[3] a) D. E. Koshland, *Science* **1963**, *142*, 1533-1541; b) D. E. Koshland, *Angew. Chem. Int. Ed.* **1994**, *33*, 2375-2378.

[4] a) S. T. Wang, T. Sawada, K. Ohara, K. Yamaguchi, M. Fujita, *Angew. Chem. Int. Ed.* **2016**, *55*, 2063-2066; b) S. Hiraoka, K. Harano, T. Nakamura, M. Shiro, M. Shionoya, *Angew. Chem. Int. Ed.* **2009**, *48*, 7006-7009; c) K. Kasai, M. Aoyagi, M. Fujita, *J. Am. Chem. Soc.* **2000**, *122*, 2140-2141; d) Y. Y. Zhan, T. Kojima, T. Nakamura, T. Takahashi, S. Takahashi, Y. Haketa, Y. Shoji, H. Maeda, T. Fukushima, S. Hiraoka, *Nat. Commun.* **2018**, *9*.

[5] T. Sawada, H. Hisada, M. Fujita, *J. Am. Chem. Soc.* **2014**, *136*, 4449-4451.

[6] a) V. Martinez-Agramunt, E. Peris, *Inorg. Chem.* **2019**, *58*, 11836-11842; b) V. Martinez-Agramunt, T. Eder, H. Darmandeh, G. Guisado-Barrios, E. Peris, *Angew. Chem. Int. Ed.* **2019**, *58*, 5682-5686; c) V. Martinez-Agramunt, D. Gusev, E. Peris, *Chem. Eur. J.* **2018**, *24*, 14802-14807; d) V. Martinez-Agramunt, S. Ruiz-Botella, E. Peris, *Chem. Eur. J.* **2017**, *23*, 6675-6681; e) V. Martínez-Agramunt, E. Peris, *Chem. Commun.* **2019**, DOI: 10.1039/c1039cc08595e.

[7] a) X. M. Chang, Z. X. Zhou, C. D. Shang, G. Wang, Z. L. Wang, Y. Y. Qi, Z. Y. Li, H. Wang, L. P. Cao, X. P. Li, Y. Fang, P. J. Stang, *J. Am. Chem. Soc.* **2019**, *141*, 1757-1765; b) N. W. Wu, J. Zhang, D. Ciren, Q. Han, L. J. Chen, L. Xu, H. B. Yang, *Organometallics* **2013**, *32*, 2536-2545; c) T. K. Ronson, W. J. Meng, J. R. Nitschke, *J. Am. Chem. Soc.* **2017**, *139*, 9698-9707.

[8] a) C. Biz, S. Ibañez, M. Poyatos, D. Gusev, E. Peris, *Chem. Eur. J.* **2017**, *23*, 14439-14444; b) S. Ibañez, E. Peris, *Angew. Chem. Int. Ed.* **2019**, *58*, 6693-6697.

[9] a) I. J. Keyte, R. M. Harrison, G. Lammel, *Chem. Soc. Rev.* **2013**, *42*, 9333-9391; b) A. K. Haritash, C. P. Kaushik, *J. Hazard. Mater.* **2009**, *169*, 1-15; c) C. L. Lemieux, A. B. Lambert, S. Lundstedt, M. Tysklind, P. A. White, *Environ. Toxicol. Chem.* **2008**, *27*, 978-990; d) K. Srogi, *Environmental Chemistry Letters* **2007**, *5*, 169-195; e) H. C. Yap, Y. L. Pang, S. Lim, A. Z. Abdullah, H. C. Ong, C. H. Wu, *International Journal of Environmental Science and Technology* **2019**, *16*, 601-628.

[10] a) J. K. Klosterman, Y. Yamauchi, M. Fujita, *Chem. Soc. Rev.* **2009**, *38*, 1714-1725; b) L. Zhang, L. Lin, D. Liu, Y. J. Lin, Z. H. Li, G. X. Jin, *J. Am. Chem. Soc.* **2017**, *139*, 1653-1660; c) A. Mishra, S. C. Kang, K. W. Chi, *Eur. J. Inorg. Chem.* **2013**, *2013*, 5222-5232; d) B. Therrien, *Eur. J. Inorg. Chem.* **2009**, 2445-2453; e) J. D. Crowley, I. M. Steele, B. Bosnich, *Eur. J. Inorg. Chem.* **2005**, 3907-3917; f) J. D. Crowley, B. Bosnich, *Eur. J. Inorg. Chem.* **2005**, 2015-2025; g) R. Lin, J. H. K. Yip, K. Zhang, L. L. Koh, K. Y. Wong, K. P. Ho, *J. Am. Chem. Soc.* **2004**, *126*, 15852-15869; h) E. M. Lopez-Vidal, A. Fernandez-Mato, M. D. Garcia, M. Perez-Lorenzo, C. Peinador, J. M. Quintela, *J. Org. Chem.* **2014**, *79*, 1265-1270; i) C. Alvarino, E. Pia, M. D. Garcia, V. Blanco, A. Fernandez, C. Peinador, J. M. Quintela, *Chem. Eur. J.* **2013**, *19*, 15329-15335; j) C. Peinador, E. Pia, V. Blanco, M. D. Garcia, J. M. Quintela, *Org. Lett.* **2010**, *12*, 1380-1383; k) V. Blanco, M. D. Garcia, A. Terenzi, E. Pia, A. Fernandez-Mato, C. Peinador, J. M. Quintela, *Chem. Eur. J.* **2010**, *16*, 12373-12380; l) R. Govindarajan, R. Nagarajaprakash, B. Manimaran, *Inorg. Chem.* **2015**, *54*, 10686-10694; m) M. H. Yuan, F. Weisser, B. Sarkar, A. Garci, P. Braunstein, L. Routaboul, B. Therrien, *Organometallics* **2014**, *33*, 5043-5045; n) M. D. Garcia, C. Alvarino, E. M. Lopez-Vidal, T. Rama, C. Peinador, J. M. Quintela, *Inorg. Chim. Acta* **2014**, *417*, 27-37; o) N. Kishi, Z. Li, Y. Sei, M. Akita, K. Yoza, J.

S. Siegel, M. Yoshizawa, *Chem. Eur. J.* **2013**, *19*, 6313-6320; p) K. Omoto, S. Tashiro, M. Shionoya, *Chemical Science* **2019**, *10*, 7172-7176.

[11] a) E. J. Dale, N. A. Vermeulen, A. A. Thomas, J. C. Barnes, M. Juricek, A. K. Blackburn, N. L. Strutt, A. A. Sarjeant, C. L. Stern, S. E. Denmark, J. F. Stoddart, *J. Am. Chem. Soc.* **2014**, *136*, 10669-10682; b) M. Juricek, J. C. Barnes, E. J. Dale, W. G. Liu, N. L. Strutt, C. J. Bruns, N. A. Vermeulen, K. C. Ghooray, A. A. Sarjeant, C. L. Stern, Y. Y. Botros, W. A. Goddard, J. F. Stoddart, *J. Am. Chem. Soc.* **2013**, *135*, 12736-12746; c) J. C. Barnes, M. Juricek, N. L. Strutt, M. Frasconi, S. Sampath, M. A. Giesener, P. L. McGrier, C. J. Bruns, C. L. Stern, A. A. Sarjeant, J. F. Stoddart, *J. Am. Chem. Soc.* **2013**, *135*, 183-192; d) E. J. Dale, N. A. Vermeulen, M. Juricek, J. C. Barnes, R. M. Young, M. R. Wasielewski, J. F. Stoddart, *Acc. Chem. Res.* **2016**, *49*, 262-273.

[12] a) E. Nestoros, M. C. Stuparu, *Chem. Commun.* **2018**, *54*, 6503-6519; b) X. Li, F. Y. Kang, M. Inagaki, *Small* **2016**, *12*, 3206-3223; c) Y. T. Wu, J. S. Siegel, *Chem. Rev.* **2006**, *106*, 4843-4867.

[13] M. Juricek, N. L. Strutt, J. C. Barnes, A. M. Butterfield, E. J. Dale, K. K. Baldridge, F. Stoddart, J. S. Siegel, *Nat. Chem.* **2014**, *6*, 222-228.

[14] B. M. Schmidt, T. Osuga, T. Sawada, M. Hoshino, M. Fujita, *Angew. Chem. Int. Ed.* **2016**, *55*, 1561-1564.

[15] D. Nuevo, M. Poyatos, E. Peris, *Organometallics* **2018**, *37*, 3407-3411.

[16] a) J. F. Stoddart, *Chem. Soc. Rev.* **2009**, *38*, 1802-1820; b) W. R. Dichtel, O. S. Miljanic, J. M. Spruell, J. R. Heath, J. F. Stoddart, *J. Am. Chem. Soc.* **2006**, *128*, 10388-10390; c) F. Arico, J. D. Badjic, S. J. Cantrill, A. H. Flood, K. C. F. Leung, Y. Liu, J. F. Stoddart, in *Templates in Chemistry Ii, Vol. 249* (Eds.: C. A. Schalley, F. Vogtle, K. H. Dotz), **2005**, pp. 203-259.

[17] J. C. Hanson, C. E. Nordman, *Acta Crystallographica Section B-Structural Science* **1976**, *32*, 1147-1153.

[18] Z. F. Yao, J. Y. Wang, J. Pei, *Cryst. Growth. Des.* **2018**, *18*, 7-15.

[19] a) A. J. Lowe, F. M. Pfeffer, P. Thordarson, *Supramol. Chem.* **2012**, *24*, 585-594; b) P. Thordarson, *Chem. Soc. Rev.* **2011**, *40*, 1305-1323.

Entry for the Table of Contents

COMMUNICATION

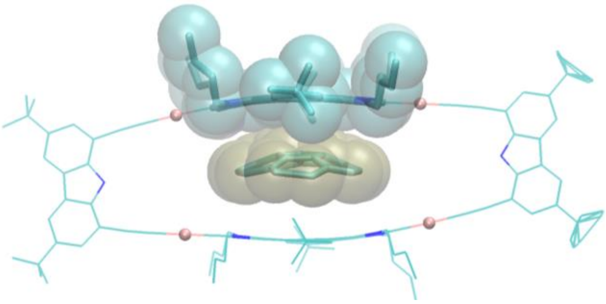

Corannulene and metallorectangle are mutually adapted to maximize shape complementarity upon formation of a host:guest complex

*Susana Ibáñez and Eduardo Peris**

Page No. – Page No.

Dimensional matching *vs*. induced-fit distortions. Binding affinities of planar and curved polyaromatic hydrocarbons with a tetra-gold metallorectangle